ORIGINAL ARTICLE

Journal of Cachexia, Sarcopenia and Muscle 2021; **12**: 1597–1612
Published online 19 October 2021 in Wiley Online Library (wileyonlinelibrary.com) **DOI:** 10.1002/jcsm.12795

Loss of REDD1 prevents chemotherapy-induced muscle atrophy and weakness in mice

Brian A. Hain, Haifang Xu & David L. Waning*

Dept. of Cellular and Molecular Physiology, The Penn State College of Medicine, Hershey, PA, USA

Abstract

Background Chemotherapy is an essential treatment to combat solid tumours and mitigate metastasis. Chemotherapy causes side effects including muscle wasting and weakness. Regulated in Development and DNA Damage Response 1 (REDD1) is a stress-response protein that represses the mechanistic target of rapamycin (mTOR) in complex 1 (mTORC1), and its expression is increased in models of muscle wasting. The aim of this study was to determine if deletion of REDD1 is sufficient to attenuate chemotherapy-induced muscle wasting and weakness in mice.

Methods C2C12 myotubes were treated with carboplatin, and changes in myotube diameter were measured. Protein synthesis was measured by puromycin incorporation, and REDD1 mRNA and protein expression were analysed in myotubes treated with carboplatin. Markers of mTORC1 signalling were measured by western blot. REDD1 global knockout mice and wild-type mice were treated with a single dose of carboplatin and euthanized 7 days later. Body weight, hindlimb muscle weights, forelimb grip strength, and extensor digitorum longus whole muscle contractility were measured in all groups. Thirty minutes prior to euthanasia, mice were injected with puromycin to measure puromycin incorporation in skeletal muscle.

Results C2C12 myotube diameter was decreased at 24 ($P = 0.0002$) and 48 h ($P < 0.0001$) after carboplatin treatment. Puromycin incorporation was decreased in myotubes treated with carboplatin for 24 ($P = 0.0068$) and 48 h ($P = 0.0008$). REDD1 mRNA and protein expression were increased with carboplatin treatment ($P = 0.0267$ and $P = 0.0015$, respectively), and this was accompanied by decreased phosphorylation of Akt T^{308} ($P < 0.0001$) and S^{473} ($P = 0.0006$), p70S6K T^{389} ($P = 0.0002$), and 4E-binding protein 1 S^{65} ($P = 0.0341$), all markers of mTORC1 activity. REDD1 mRNA expression was increased in muscles from mice treated with carboplatin ($P = 0.0295$). Loss of REDD1 reduced carboplatin-induced body weight loss ($P = 0.0013$) and prevented muscle atrophy in mice. REDD1 deletion prevented carboplatin-induced decrease of protein synthesis ($P = 0.7626$) and prevented muscle weakness.

Conclusions Carboplatin caused loss of body weight, muscle atrophy, muscle weakness, and inhibition of protein synthesis. Loss of REDD1 attenuates muscle atrophy and weakness in mice treated with carboplatin. Our study illustrates the importance of REDD1 in the regulation of muscle mass with chemotherapy treatment and may be an attractive therapeutic target to combat cachexia.

Keywords REDD1; Chemotherapy; Muscle atrophy; Muscle weakness; Protein synthesis; Cachexia

Received: 3 November 2020; Revised: 30 June 2021; Accepted: 23 August 2021
**Correspondence to: David L. Waning, Dept. of Cellular and Molecular Physiology, The Penn State College of Medicine, 500 University Drive, H166, Rm C4718E, Hershey, PA 17033, USA, Phone: 1-717-531-3853. Email: dwaning@psu.edu*

Introduction

Chemotherapy is a crucial anti-neoplastic strategy to treat malignancies in cancer patients.[1] Unfortunately, chemotherapy drugs are often accompanied by a range of side effects including muscle weakness and loss of muscle mass, which define chemotherapy-induced cachexia.[2] Greater muscle mass is associated with positive patient prognosis due to enhanced metabolic activity[2,3] and also limits chemotherapy toxicity, reducing the severity of a number of side effects.[4] Many studies have now shown that chemotherapy treatment itself can lead to loss of muscle mass and muscle weakness.[5–9]

Carboplatin is a platinum-based chemotherapy drug that cross-links DNA leading to cell death[10] and also causes muscle atrophy and muscle weakness.[8,9] Various studies have demonstrated that platinum-based chemotherapy treatments induce loss of muscle mass in both animal models[9,11,12] and humans.[13] In both *in vivo* and *in vitro* studies, an increase in protein degradation has been associated with chemotherapy treatment including increased expression of the E3 ubiquitin ligases, muscle RING-finger 1 (MuRF1)[14] and MAFbx (atrogin-1).[9,15] While the bulk of research concerning chemotherapy-induced loss of muscle mass has been conducted investigating catabolic pathways, anabolic signalling is also compromised. Doxorubicin causes loss of muscle mass, decreased exercise capacity, and decreased protein synthesis in mice.[16] Cisplatin causes decreased phosphorylation of protein kinase B (Akt)[17] and decreased IGF-1 gene expression,[11] both upstream regulators of protein synthesis. Folfiri, a chemotherapy cocktail, causes activation of the extracellular signal-related kinase 1/2 (ERK1/2) and p38 MAPK signalling pathways and causes muscle atrophy and weakness.[7]

Maintenance of muscle mass is multifaceted, and muscle size is dependent upon the balance of rates of protein synthesis and protein degradation.[18,19] During periods of muscle wasting, this balance shifts towards an increase in protein degradation and a decrease in protein synthesis leading to muscle atrophy.[20] A key negative regulator of protein synthesis is the stress-response protein Regulated in Development and DNA Damage Response 1 (REDD1; also known as DDIT4).[21] Genetic knockout of REDD1 is sufficient to maintain skeletal muscle protein synthesis in a variety of pathophysiological conditions in mice including fasting,[22] sepsis,[23] and hypoxia,[24] and enhances muscle hypertrophy.[25] Because chemotherapy results in muscle wasting and muscle weakness, maintaining protein synthesis would be expected to prevent loss of muscle mass and enhance a patient's prognosis due to advanced cancer and cancer treatment.

Under non-stress physiological conditions, REDD1 is not highly expressed in myofibers.[26] However, REDD1 protein expression is upregulated in hypoxic conditions by hypoxia inducible factor 1 alpha[27,28] and with endoplasmic reticulum (ER) stress by activating transcription factor 4.[29] Increased expression of REDD1 inhibits mechanistic target of rapamycin in complex 1 (mTORC1) activity and subsequent downstream protein translation/synthesis.[21,30] The PI3K/Akt/mTOR pathway has been extensively studied, and mTORC1 activation is partially reliant on active Akt and adequate growth conditions.[22] Through a series of intermediate phosphorylation events, Akt activates mTORC1 in a ras homolog enriched in brain-dependent manner.[31] mTORC1 then phosphorylates downstream targets ribosomal protein S6 kinase beta-1 and eukaryotic translation initiation factor 4E-binding protein 1 allowing increased protein translation to occur.[32] Previous studies have elucidated two mechanisms of action of REDD1 in the modulation of mTORC1 activity. Dennis *et al*. presented evidence that REDD1 enhances protein phosphatase 2A activity, thereby enhancing the dephosphorylation of Akt on threonine 308 leading to decreased mTORC1 activation in HEK-293 cells.[33] Ellison *et al*. demonstrate that under hypoxic conditions, REDD1 interacts with the tuberous sclerosis tumour suppressors, specifically tuberin (TSC2), binding to 14-3-3 allowing TSC2 to complex with hemartin (TSC1). The TSC1/2 complex prevents the activation of mTORC1 in a ras homolog enriched in brain-dependent manner in MEF cells.[27] REDD1's mechanism of action has not been identified in skeletal muscle, and the role that REDD1 plays in modulation of muscle mass through mTORC1 regulation with chemotherapy has not been studied. However, REDD1 has been shown to be increased in muscles from mice treated with combination cyclophosphamide, doxorubicin, and 5-flurouracil treatment.[34] We hypothesize that REDD1 expression in mouse skeletal muscle is induced with carboplatin treatment and deletion of REDD1 will attenuate chemotherapy-induced muscle atrophy and muscle weakness by maintaining mTORC1-dependent protein synthesis.

Methods

Animals

Eight-week-old female REDD1 homozygous knockout (REDD1 KO) or wild-type C57bl/6 × 129SvEv mice[35] were used for the study. REDD1 KO mice are in the same genetic background as controls and were originally generated by Elena Feinstein at Quark Pharmaceuticals.[35] Food and water were provided *ad libitum* except when food was removed 3 h prior to euthanasia. Twelve-week-old female wild-type mice were used as age controls to verify loss of body mass in skeletally mature mice as confirmed by measurement of tibia length. All experiments were repeated with independent groups. All experiments using animals were performed at the Penn State College of Medicine and approved by Penn State University's Institutional Animal Care and Use Committee and have been performed in accordance with the ethical standards laid down in the 1964 Declaration of Helsinki and its later amendments.

Genotyping

Genotyping was performed using PCR on genomic DNA extracted from mouse ear clips using REDD1 2-exon specific forward (5′-CTGGGATCGTTTCTCGTCCTC-3′) and reverse (5′-CATCCAGGTATGAGGAGTCTG-3′) oligonucleotides. A neomycint-specific forward oligonucleotide (5′-GATGGATTGCACGCAGGTTC-3′) that shared the REDD1 reverse sequence was utilized to further confirm REDD1 KO.[35] Genotype for all mice was confirmed prior to experimentation.

Drugs

Carboplatin (Millipore-Sigma, Darmstadt, Germany) dissolved in phosphate buffered saline (PBS) or vehicle was injected once intraperitoneally at a dose of 100 mg/kg. This dose has been shown to closely match the area under the plasma concentration curve vs. time when compared with an equivalent human dose at a ratio of 0.9 mouse : human.[36] Mice were then returned to their cages and euthanized 5 or 7 days after injection. Body weights were monitored daily, and a loss of 20% or greater of initial body weight fulfilled endpoint criteria and required euthanasia.

Plasmid transfection in vivo

pLKO.1 (Addgene plasmid #10878[37]) (shControl), pcDNA3-EGFP (Addgene plasmid #13031), and REDD1 shRNA (shREDD1) construct TRCN0000176020 (Sigma, Darmstadt, Germany) were used for *in vivo* electroporation. Plasmid constructs were purified using an endotoxin-free maxi-prep kit (Qiagen, Hilden, Germany). 10 μg of either shControl or shREDD1 were mixed with 10 μg of GFP in a volume of 50ul of sterile PBS. Eight-week-old female wild-type mice were anesthetized using 5% isoflurane gas until surgical plane of anaesthesia was met. Isoflurane was reduced to 2% maintenance dose and absence of toe pinch reflex confirmed anaesthesia. Hair from the lower hindlimb was removed using a depilatory cream, and the injection site was scrubbed with 70% ethanol. A 50 μL Hamilton syringe with 30 gauge needle was used to inject the plasmid cocktail (left leg shControl + GFP; right leg shREDD1 + GFP). The injection site was at the distal tibialis anterior (TA), and the needle was inserted through the skin, into the TA to the proximal origin. The syringe was gently depressed while simultaneously withdrawing the needle the length of the TA to insure adequate distribution of the constructs. After 1 min calliper electrodes were placed medially and laterally around the lower hindlimb in the area of the TA and 5 pulses at 125 V/cm at 20 ms duration, 200 ms intervals were delivered using an electroporator (BTX, Holliston, MA). Forty-eight hours later, mice were injected with carboplatin and euthanized 5 days later as previously described. When skeletal muscle is injected with a mixture containing two vectors, co-transfection of a myofibre occurs 75–95% of the time.[38,39]

Forelimb grip strength

Forelimb grip strength was assessed by allowing each mouse to grasp a wire mesh attached to a force transducer (Bioseb, Vitrolles, France) that records peak force generated as the mouse is pulled by the base of the tail horizontally away from the mesh.[40] We performed three consecutive pulls separated by 5 s pauses between each pull. Absolute grip strength (grammes) was calculated as the average of the peak forces from the three pulls. The investigators were blinded to treatment of the subjects.

Cell culture

C2C12 myoblasts (CRL-1772, ATCC, Manassas, VA) were cultured subconfluently in Dulbecco's modified Eagle's media (DMEM) (Hyclone, Logan, UT) with 10% foetal bovine serum (VWR, Radner, PA). Differentiation to myotubes was initiated by replacing growth media with Dulbecco's modified Eagle's media supplemented with 2% horse serum (Hyclone) plus 1% foetal bovine serum for 4 days, refreshing media every 48 h. Three-hundred-micromolar carboplatin was diluted in differentiation media and applied to cells for 24 or 48 h prior to harvest. Three hundred micromolars was the lowest effective dose to induce myotube atrophy. Another set of myoblasts were differentiated for 6 days before carboplatin treatment as described above to confirm effects in myotubes under extended differentiation. Cells were maintained at 37°C with 5% CO_2 in a humidified chamber. Three biological replicates were used for analysis, and all experiments were repeated at least twice to confirm findings.

Plasmid transfection in vitro

Six-day differentiated C2C12 myotubes were incubated with 20 μg of both shControl and GFP plasmid or 20 μg of both shREDD1 and GFP (as described above) in differentiation media for 5 min. Myotubes were then electroporated using a BTX Petri Pulsor (BTX, Holliston, MA) for 5 pulses at 175 V/cm, 20 ms duration with 200 ms interval. After electroporation, media was aspirated, and fresh differentiation media was applied. Twenty-four hours later, myotubes were treated with carboplatin for 24 h as described previously. Three biological replicates were used for analysis, and all experiments were repeated at least twice to confirm findings.

Protein synthesis

Mice in the 5 day group were injected intraperitoneally with 0.040 μmol/g bodyweight of puromycin (Tocris Bioscience, Bristol, UK) dissolved in 100 μL PBS exactly 30 min prior to euthanasia for puromycin incorporation measurements to assess protein synthesis. Access to food was removed 3 h prior to euthanasia in order to control for nutrient uptake variability in protein synthesis measurements.[41] C2C12 myotubes were treated with 1 μM puromycin diluted in differentiation media for 30 min prior to harvest to assess protein synthesis *in vitro*.

Tissue

Mice were euthanized and the TA, soleus, and gastrocnemius were dissected. The extensor digitorum longus (EDL) muscle was dissected for muscle contractility. Muscles were either snap frozen in liquid nitrogen for biochemical analysis or embedded in optimal cutting temperature compound (Sakura Finetek, Torrance, CA, USA) in cryomolds and frozen in liquid nitrogen-cooled 2-methylbutane (isopentane) for histological analysis.[40] The EDL was snap frozen in liquid nitrogen after contractility testing. Muscle tissue was stored at −80°C.

Muscle function

Whole muscle contractility of the EDL muscle was determined as previously described.[42] Briefly, the EDL was dissected from the hindlimbs, and custom stainless-steel hooks were tied to the tendons of the muscles using 4–0 silk sutures, and the muscles were mounted between a force transducer (Aurora Scientific, Aurora, Canada) and an adjustable hook. The muscles were immersed in a tissue bath with bubbled O_2 (100%) in Tyrode solution (121 mM NaCl, 5.0 mM KCl, 1.8 mM $CaCl_2$, 0.5 mM $MgCl_2$, 0.4 mM NaH_2PO_4, 24 mM $NaHCO_3$, 0.1 mM EDTA, 5.5 mM glucose). The muscle was stimulated to contract using supramaximal stimulus between two platinum electrodes. Data were collected via Dynamic Muscle Control/Data Acquisition and Dynamic Muscle Control Data Analysis programmes (Aurora Scientific). At the start of each experiment, the muscle length was adjusted to yield the maximum force. The force–frequency relationships were determined by triggering contraction using incremental stimulation frequencies (0.5 ms pulses at 1–150 Hz for 350 ms at supramaximal voltage). Between stimulations, the muscle was allowed to rest for 3 min. At the end of the force measurement, the length (L_0) and weight of the muscle was measured. To quantify the specific force, the absolute force was normalized to the muscle size, specifically cross-sectional area (CSA), calculated as the muscle weight divided by the length using a muscle density constant of 1.056 kg/m^{-3}.[43] The investigators were blinded to treatment of the subjects.

Histology

Transverse muscle sections (10 μm) were sliced with a cryostat microtome (Microm HM 505E, GMI, Ramsey, MN, USA) from the proximal belly of the TA and fixed in 4% paraformaldehyde. The muscle sections were incubated with wheat germ agglutinin conjugated to Texas Red-X (Thermo Fisher Scientific, Waltham, MA, USA) diluted in PBS for visualization of muscle fibres under fluorescence microscopy (excitation wavelength: 596 nm; emission wavelength 615 nm). Images were captured with an AxioCam 503 mono (Zeiss, Oberkochen, Germany) using a Photofluor LM75 metal-halide light source (89 North, Patchogue, NY, USA). Three 20× magnification images per muscle were analysed for myofibre CSA (~200 fibres) using automated MyoVision software (University of Kentucky) as previously described.[44] Transverse muscle sections (10 μm) were used for immunofluorescent determination of myosin heavy chain (MyHC) fibre type as previously described.[40] Briefly, TA muscle sections were blocked for 1 h in 10% normal goat serum (NGS) and briefly washed in PBS. Slides were incubated overnight at 4°C with primary antibodies for anti-MyHCI, anti-MyHCIIa, and anti-MyCHIIb diluted in 10% NGS. The BA-D5, SC-71, and BF-F3 monoclonal antibodies, respectively, were obtained from the Developmental Studies Hybridoma Bank, created by the NICHD of the NIH and maintained at The University of Iowa, Department of Biology, Iowa City, IA 52242. Slides were then washed three times in 5 min in PBS and incubated for 1 h in the dark with goat anti-mouse secondary antibodies IgG2b Alex Fluor 350, IgG1 Alexa Fluor 594, and IgM Alexa Fluor 488 (Life Technologies, Carlsbad, CA, USA) diluted in 10% NGS. Four 20× magnification images were captured per section using the same camera and light source listed above (excitation 350, 488, and 596 nm). Images from each wavelength were merged, and muscle fibres were counted. MyHCI fibres appear blue, MyHCIIa fibres appear red, MyHCIIb fibres appear green, and MyHCIIx fibres are unstained and appear black. Data are expressed a percent of each fibre type to total number of fibres. Cross sections from TA muscles from wild-type mice transfected with shControl + GFP or shREDD1 + GFP were produced as previously described. Ten micromolar muscle sections were stained with wheat germ agglutinin conjugated to Texas Red to visualize individual myofibres. To visualize GFP positive myofibres, sections were exposed to 488 nm wavelength light, and images were captured as described previously. GFP positive myotubes appear green while GFP negative fibres are black. CSA for GFP positive myofibres were measured as previously described. C2C12 myotubes were fixed in 4% PFA for 10 min. Myotubes were blocked in 8% BSA + 1% saponin diluted in PBS for 1 h followed by overnight incubation in blocking buffer plus anti-MyHC primary antibody at 1:100 dilution at 4°C. Cells were washed 3 × 5 min in cold PBS and incubated for 1 h in blocking buffer with Alexa Fluor 488 goat anti-mouse 1gG2b

in the dark at room temperature. Cells were then washed 3 × 5 min in cold PBS and imaged as described above. C2C12 myotubes transfected with experimental plasmids were not fixed, and images were taken at 488 nm excitation wavelength. GFP positive cells appear green. Myotube diameter was analysed using Image J software, measuring the thinnest area of individual myotubes. Approximately 150 myotubes per well were measured from three wells per group. All measurements were calculated from three biological replicates and repeated at least twice. Staff was blinded to groups.

Western blotting

Tibialis anterior or gastrocnemius muscle was lysed using a Dounce homogenizer in NP-40 lysis buffer (50 mM Tris pH 8.0, 150 mM NaCl, 1% NP-40) with cOmplete Mini, EDTA-free protease inhibitors (Millipore-Sigma, Darmstadt, Germany) and phosphatase inhibitors (1 mM Na_3OV_4; 5 mM NaF). Samples were centrifuged at 5000*g* for 15 min to remove cell debris, and the supernatant was collected and stored at −80°C. Protein concentration of muscle homogenates was determined by Bradford (Bio-Rad). Samples were diluted in loading buffer (62.5 mM Tris HCl pH 6.8, 2.5% SDS, 0.002% Bromophenol Blue, 0.7135 M β-mercaptoethanol, 10% glycerol) and heat denatured. Equal amounts of protein were separated using SDS-PAGE. Proteins were transferred for 60 min at 100 V onto an immobilon-FL polyvinylidene fluoride membrane (Millipore-Sigma, Darmstadt, Germany) and incubated in Revert solution (LI-COR Biosciences, Lincoln, NE, USA) for 5 min. The membrane was imaged using an Odyssey cLX infrared imaging system (LI-COR, Lincoln, NE, USA) to quantify total protein. The membrane was then washed with Revert wash solution (LI-COR, Lincoln, NE, USA), blocked in Licor blocking buffer (LI-COR, Lincoln, NE, USA) for 1 h, and incubated overnight with primary antibody diluted in blocking buffer. Refer to the supporting information for the list of primary antibodies (Supporting Information, *Table S1*). After washing, the membranes were incubated with secondary antibodies (LI-COR Biosciences, Lincoln, NE, USA) and visualized again using the Odyssey cLX infrared imaging system. Relative quantification of proteins was determined by measuring the fluorescence of each lane at the appropriate molecular weight and normalized to total protein.

Semi-quantitative real-time PCR

Tibialis anterior or gastrocnemius muscle was lysed using a Bullet Blender Storm 24 bead homogenizer (Next Advance, Troy, NY, USA) in Trizol (Thermo Fisher, Waltham, MA, USA) for RNA extraction. One-fifth volume chloroform was added to lysates and vortexed vigorously for 15 s and incubated at room temperature for 3 min. Samples were centrifuged (12 000*g*, 15 min, 4°C), and the upper aqueous phase was collected and loaded onto a GenElute mammalian total RNA mini column (Millipore-Sigma, Darmstadt, Germany). Total RNA was isolated according to manufacturer's instructions. DNase I treatment was performed to remove genomic DNA contamination (Qiagen, Hilden, Germany). RNA quantity was determined using a Nanodrop 2000 spectrophotometer (Thermo Scientific, Waltham, MA, USA), and RNA (500 ng per sample) was reverse transcribed using Superscript II (Thermo Fisher, Waltham, MA, USA) according to the manufacturer's instructions with anchored oligo (dT) (Promega, Madison, WI, USA). The resulting complementary DNAs were prepared for real-time PCR using HotStart-IT SYBR Green PCR Kit (Thermo Fisher, Waltham, MA, USA) and oligos listed below. All targets were analysed using QuantStudio 3 Real-Time PCR System (Thermo Fisher, Waltham, MA, USA). SYBR Green primers were optimized for real-time PCR (amplification efficiency 100 ± 5%) and amplified 40 cycles (95°C for 15 s, 58°C 30 s, 72°C for 30 s) after an initial 2 min incubation at 95°C. Target gene expression (*REDD1 and REDD2*) was normalized against the housekeeping genes *β2-microglobulin (B2M)* or *ribosomal protein L32* (*RPL32)*, and data were analysed using the $\Delta\Delta Ct$ method. Primer sequences are included in (*Table S2*). The investigators were blinded to treatment of the subjects.

Protein carbonyl assay

Protein oxidative modifications were measured by protein carbonyl quantitation using a commercially available colorimetric assay (Cayman Chemical, Ann Arbor, MI, USA; Cat#10005020). Briefly, 200 mg of rectus femoris muscle or C2C12 myotubes from 3 cm dishes were homogenized in Tris-EDTA buffer (10 mM Tris, 1 mM EDTA, pH 6.8). Absorbance was measured at 360 nm wavelength on a plate reader. Protein carbonylation was normalized to protein amount (mg of tissue) for muscle lysates.

Statistical analysis

Data were analysed with the use of GraphPad Prism v7.0d software (GraphPad, San Diego, CA, USA). All results were expressed as mean ± SD, and $P < 0.05$ was considered significant.

Results

Carboplatin-induced atrophy, increased REDD1 expression, and induced oxidative stress in C2C12 myotubes. Carboplatin causes skeletal muscle atrophy in mice.[8,9] To further

investigate carboplatin-induced muscle atrophy, we treated C2C12 myotubes differentiated for either 4 or 6 days with carboplatin and measured myotube diameter. We found that C2C12 myotubes treated with carboplatin exhibited a decrease in myotube diameter after 24 h that progressed at 48 h of carboplatin treatment (*Figure 1A*). Myotubes at 4 days of differentiation were used for all further experiments. Maintenance of muscle mass is dependent on the balance between protein synthesis and protein degradation. Because REDD1 is an important regulator of mTORC1 activity, we measured REDD1 mRNA and protein in C2C12 myotubes treated with carboplatin. C2C12 myotubes treated with carboplatin had increased REDD1 mRNA and REDD1 protein (*Figure 1B–C*). Myotubes treated with carboplatin for 24 h also had increased protein carbonylation, a marker of oxidative stress (*Figure S1A*). Our data show that carboplatin causes myotube atrophy, increased oxidative stress, and increased REDD1 expression.

Carboplatin reduced protein synthesis in C2C12 myotubes. REDD1 regulates mTORC1 activity so we measured incorporation of puromycin into growing polypeptide chains to assess protein synthesis. Incorporation of puromycin into the polypeptide prevents elongation and leads to puromycin bound truncation products that are released from the ribosome. Puromycin was then measured by western blot. C2C12 myotubes treated with carboplatin for 24 and 48 h were incubated with puromycin exactly 30 min prior to harvesting the cells. Myotubes treated with carboplatin had reduced puromycin incorporation at both 24 and 48 h (*Figure 2A*) suggesting that protein synthesis is reduced in carboplatin-treated

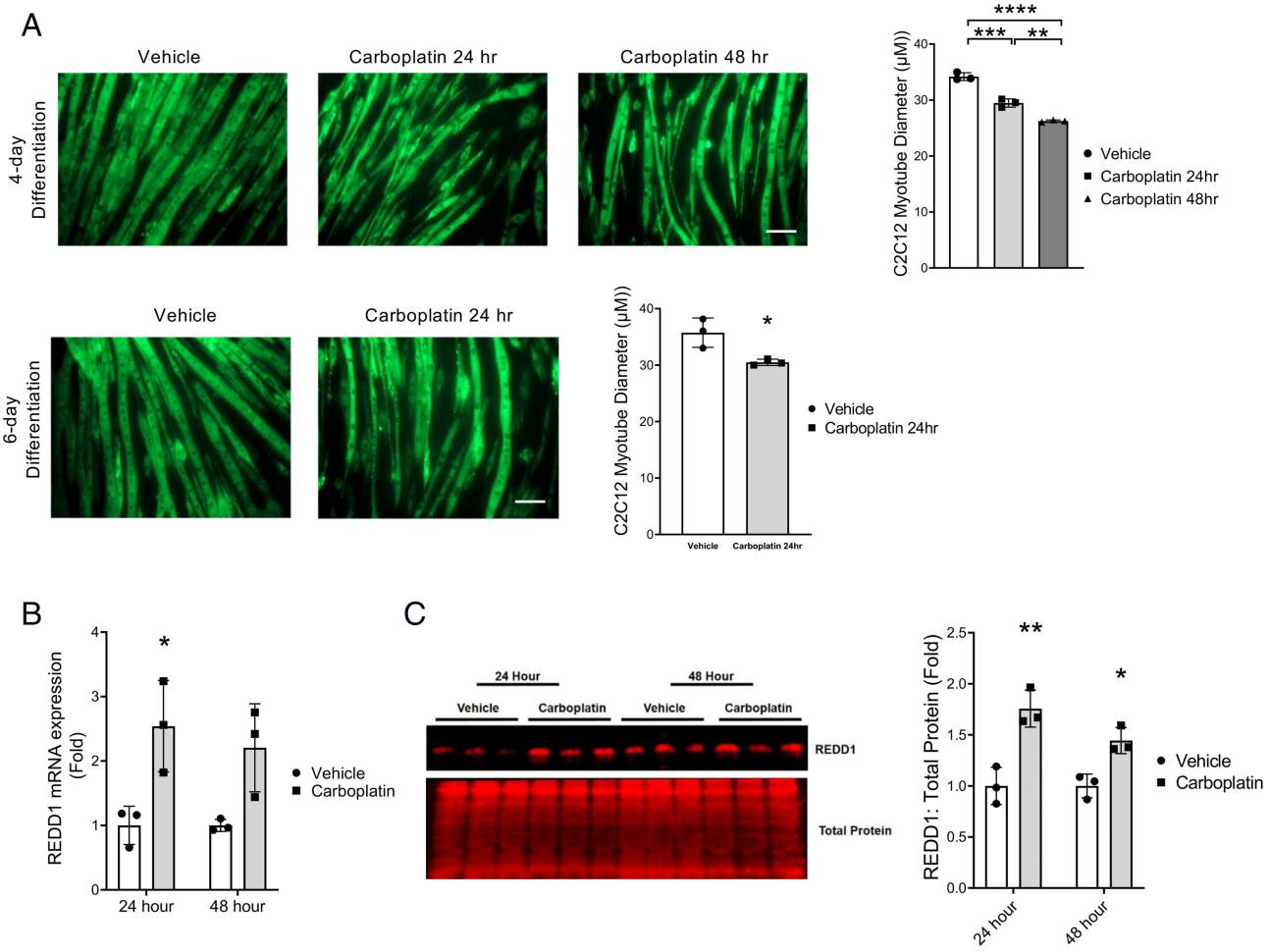

Figure 1 Carboplatin caused C2C12 myotube atrophy and increased REDD1 expression. C2C12 myotubes were treated with carboplatin for 24 or 48 h. (*A*) C2C12 myotube diameter was decreased after carboplatin treatment compared with vehicle in C2C12 cells differentiated for either 4 or 6 days. Scale bar = 50 μm. (*B*) REDD1 mRNA expression was increased in C2C12 myotubes differentiation for 4 days and treated with carboplatin for either 24 or 48 h. (*C*) REDD1 protein expression was increased in C2C12 myotubes differentiation for 4 days and treated with carboplatin for either 24 or 48 h. (*A*) One-way ANOVA with Tukey's post-hoc test for multiple comparisons, or Student's *t*-test. (*B–C*) Two-way ANOVA with Tukey's post-hoc test for multiple comparisons. $*P < .05$ $**P < 0.01$, $***P < 0.001$, $****P < 0.0001$. (*A*) Approximately 100 myotubes assessed, $n = 3$ biological replicates for all groups. (*B–C*) $n = 3$ biological replicates for all groups.

DOI: 10.1002/jcsm.12795

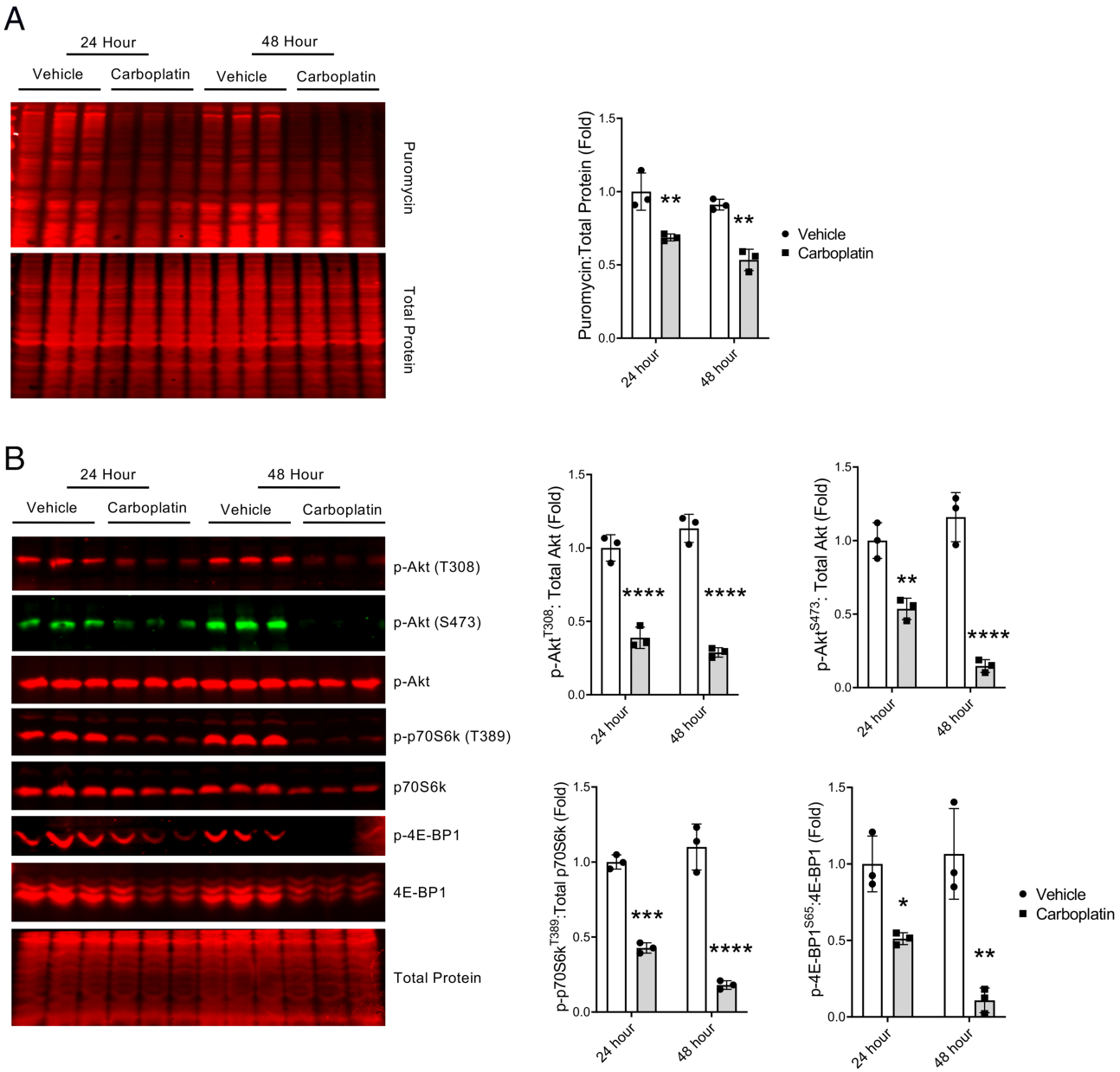

Figure 2 Carboplatin reduced protein synthesis and decreased markers of mTORC1 activation in C2C12 myotubes. (*A*) C2C12 myotubes treated with carboplatin for either 24 or 48 h and incubated with puromycin for 30 min before harvest. Incorporation of puromycin was measured by western blot and quantitated to show decreased puromycin incorporation into growing peptide chains. (*B*) C2C12 myotubes treated with carboplatin for either 24 or 48 h were used to measure phosphorylation of Akt at threonine 308 and serine 473. Phosphorylation of p70S6K at threonine 389 and phosphorylation of 4E-BP1 at serine 65 were measured by western blot and quantitated. (*A–B*) Two-way ANOVA with Tukey's post-hoc test for multiple comparisons. $^{*}P < 0.05$ $^{**}P < 0.01$, $^{***}P < 0.001$, $^{****}P < 0.0001$. $n = 3$ biological replicates for all groups.

cells. Because mTORC1 signalling is crucial for protein synthesis, we measured markers of mTORC1 activation in myotubes treated with carboplatin for 24 and 48 h. Akt dephosphorylation (threonine 308 and serine 473) was observed at both 24 and 48 h. Downstream markers of mTORC1 activation were also dephosphorylated, 4E-binding protein 1 (serine 65) and p70S6k (threonine 389), further evidence that carboplatin caused a reduction in mTORC1 activation (*Figure 2B*). Caspase 3 and cleaved caspase 3 was measured as a marker of cytotoxicity in cells and only carboplatin-treated cells for 48 h showed any increase caspase 3 cleavage (*Figure S1B*). C2C12 myotubes were treated with 10 μM staurosporine for 6 h as a positive control for caspase 3 cleavage (*Figure S1C*). The increase of REDD1 expression and concomitant decrease of markers of mTORC1 activity and puromycin incorporation in carboplatin-treated myotubes supports

previous studies that show REDD1's negative influence on anabolic signalling.

Loss of REDD1 attenuates carboplatin-induced cachexia. REDD1 KO (C57bl/6 × 129SvEv) were used to investigate the role of REDD1 on skeletal muscle of mice treated with carboplatin. Female wild-type mice were injected with carboplatin and euthanized 7 days later. mRNA expression from the gastrocnemius muscle was increased three-fold compared with vehicle-treated wild-type mice (*Figure 3A*). REDD2 mRNA expression was also measured to assess whether or not there was a compensatory increase in REDD2, but we found no change (*Figure S2A*). REDD1 deletion was confirmed by genotype PCR for all animals in the study (*Figure S2B*), and these whole-body knockout mice and wild-type controls were used for all *in vivo* studies.

Previous studies by our lab demonstrated that carboplatin caused skeletal muscle atrophy in mice.[9] In this study, wild-type mice treated with carboplatin lose body weight over 7 days whereas weight loss in REDD1 KO mice treated with carboplatin was reduced (*Figure 3B*). We also measured carboplatin-induced weight loss in female 12-week-old mice to confirm that weight loss was not due to the age of treated mice (*Figure S3A*). Muscles from the hindlimb were carefully excised, blotted dry, and weighed at euthanasia to evaluate changes in muscle mass. The TA, gastrocnemius, EDL and soleus muscles from wild-type mice treated with carboplatin weighed less compared with vehicle-treated wild-type mice, and this loss of muscle mass was completely abolished in REDD KO mice treated with carboplatin (*Figure 3C*). Inguinal white adipose tissue was also weighed, and we found no significant differences between any groups (*Figure S3B*). These data show that loss of REDD1 in mice prevents carboplatin-induced loss of body and muscle mass.

Loss of REDD1 prevents carboplatin-induced loss of muscle cross-sectional

We investigated skeletal muscle fibre CSA in wild-type and REDD1 KO mice treated with carboplatin as well as muscle fibre type (MyHC). Three TA muscles from each group were cryo-sectioned for CSA analysis. Similar to changes in muscle weight, CSA was decreased in wild-type mice treated with carboplatin compared with vehicle-treated mice, and TA

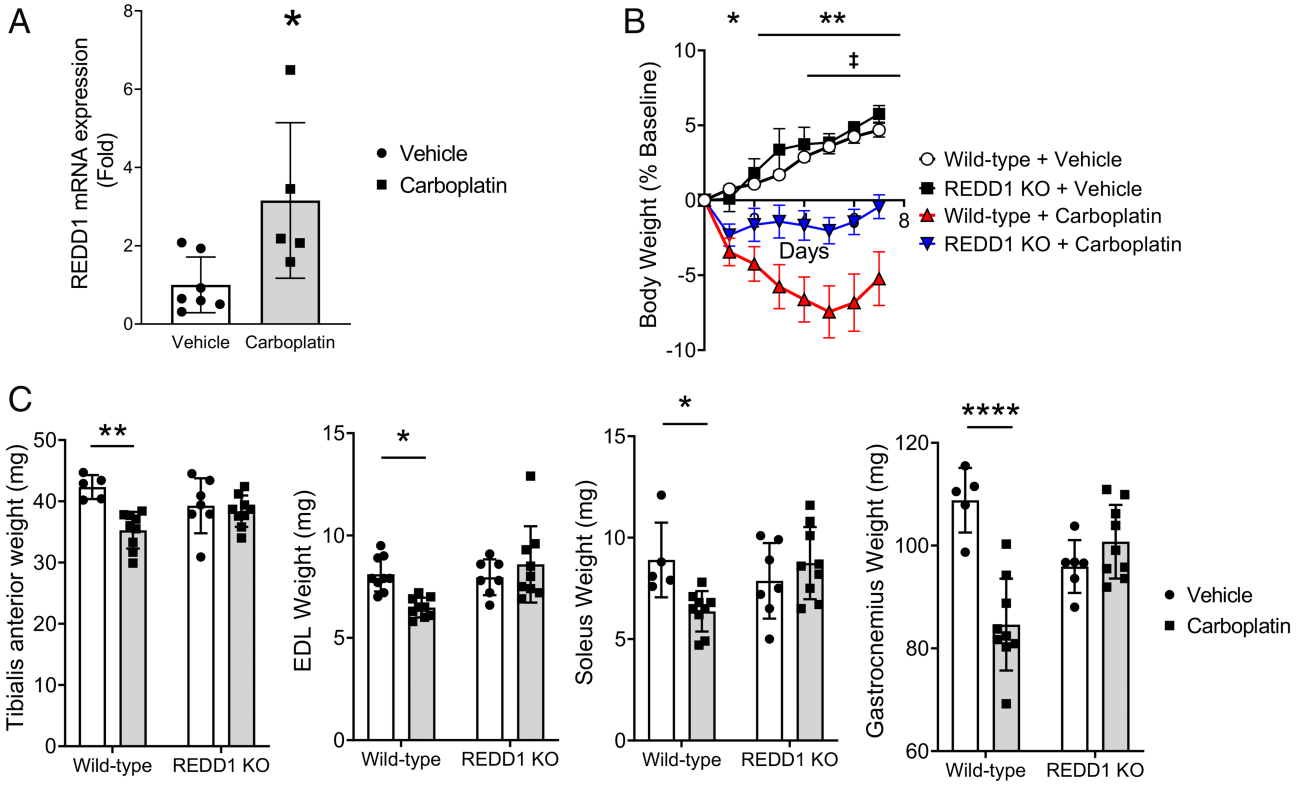

Figure 3 Loss of REDD1 *in vivo* attenuates carboplatin-induced cachexia. (*A*) REDD1 mRNA expression in the TA muscle of wild-type or REDD1 knockout (REDD1 KO) mice treated with carboplatin. (*B*) Whole animal body weight of mice treated with vehicle or carboplatin. (*C*) Weight of the TA, gastrocnemius, EDL and soleus muscles of mice treated with vehicle or carboplatin. (*A*) Student's *t*-test $^{*}P < 0.05$. (*B–C*) Two-way ANOVA with Tukey's post-hoc test for multiple comparisons. (*B*) $^{*}P < 0.05$, $^{**}P < 0.01$ wild-type + vehicle compared with wild-type + carboplatin; $^{‡}P < 0.05$ wild-type + carboplatin compared with REDD1 KO + carboplatin. (*C*)$^{*}P < 0.05$, $^{**}P < 0.01$, $^{****}P < 0.0001$. *n* = 8 biological replicates for each group (*A–C*).

DOI: 10.1002/jcsm.12795

CSA was completely preserved in REDD1 KO mice treated with carboplatin (*Figure 4A*). We also performed a myofibre CSA frequency distribution analysis and found a leftward shift in myofibre CSA from wild-type mice treated with carboplatin indicating a shift to smaller fibres. This shift was prevented in REDD1 KO mice treated with carboplatin (*Figure 4B*). Fibre-type analysis was performed through immunohistochemistry to identify the predominant MyHC per fibre. We found that there was a trending, but not significant, shift in the proportion of MyHCIIa:MyHCIIb positive fibres (fast shift) in the TA from wild-type mice treated with carboplatin that was absent in muscles from REDD1 KO mice treated with

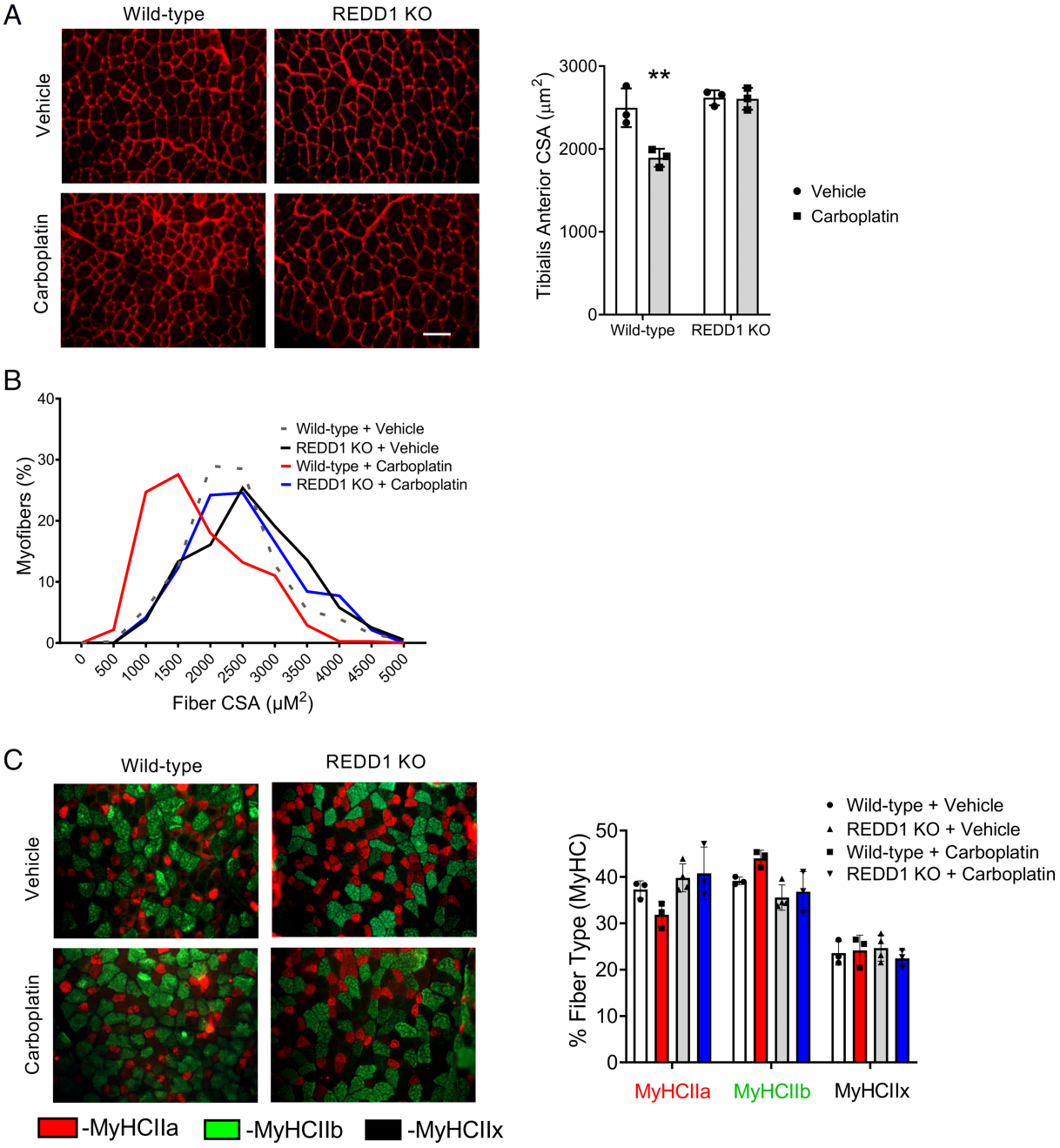

Figure 4 Loss of REDD1 prevents carboplatin-induced myofibre atrophy. (*A*) Representative cross sections and CSA quantification from the TA muscle of mice treated with vehicle or carboplatin. Scale bar = 50 μm. (*B*) Myofibre distribution frequency from the TA muscle of mice treated with vehicle or carboplatin. (*C*) Representative cross sections and quantification of MyHC fibre type from the TA muscle of mice treated with vehicle or carboplatin. (*A*, *C*) Two-way ANOVA with Tukey's post-hoc test for multiple comparisons. $^{**}P < 0.01$. $n = 3$ biological replicates for (*A*–*C*). Average CSA from ~200 fibres per replicate for (*A*–*B*) and fibre-type quantitation (*C*).

DOI: 10.1002/jcsm.12795

carboplatin (*Figure 4C*). These data show that loss of REDD1 in mice prevents carboplatin-induced muscle atrophy and this is not fibre-type dependent.

Loss of REDD1 attenuates carboplatin-induced reduction in protein synthesis. Incorporation of puromycin was used as a non-radioactive assay to measure protein synthesis in skeletal muscle *in vivo*.[45,46] At low doses, puromycin can be used to evaluate the quantity of truncated peptide strands, which reflects the rate of protein synthesis at the time of incorporation.[45] On the basis of the body weight data collected in this study, we determined that loss of body mass peaked at 5 days after carboplatin injection (*Figure 3B*). We therefore treated mice with carboplatin and euthanized 5 days later in order evaluate peak changes in protein synthesis. We injected puromycin exactly 30 min prior to euthanasia then excised the muscles for puromycin incorporation measurements. We found that wild-type mice treated with carboplatin had lower puromycin incorporation compared with vehicle-treated mice. In contrast, REDD1 KO mice did not exhibit reduced puromycin incorporation in muscles, although overall puromycin incorporation was decreased in vehicle-treated REDD1 KO mice compared with wild-type mice (*Figure 5*). The decreased puromycin incorporation in carboplatin-treated wild-type mice suggests a lower rate of protein synthesis, which is prevented in mice lacking REDD1. We measured protein carbonylation in skeletal muscle as a way to assess oxidative stress. We found that carboplatin increases carbonylated proteins in both wild-type and REDD1 KO mice, suggesting that lack of REDD1 does not change the oxidative stress induced by carboplatin and that the benefit of REDD1 KO in protection of muscle mass is independent of protein oxidation (*Figure S3C*).

Knockdown of REDD1 in C2C12 myotubes and mouse TA attenuates carboplatin-induced atrophy. Because global knockout of REDD1 may have effects in other tissues that could indirectly cause changes in skeletal muscle, we knocked down REDD1 expression specifically in C2C12 myotubes and in the TA of wild-type mice. REDD1 shRNA (shREDD1) or control shRNA (shControl) were co-electroporated with GFP in order to visualize transfected fibres. C2C12 myotubes were incubated with plasmid constructs in normal differentiation media and electroporated. 24 h later myotubes were incubated with carboplatin for 24 h. GFP positive myotubes were then imaged, and myotube diameter of green myotubes only was measured. Myotubes electroporated with shControl and treated with carboplatin had reduced myotube diameter that was attenuated in fibres electroporated with shREDD1 (*Figure 6A*). REDD1 mRNA expression was measured in C2C12 cells. REDD1 mRNA expression exhibited an increasing trend ($P = 0.0581$) in myotubes electroporated with shControl (*Figure 6B*). To determine muscle atrophy *in vivo*, we injected and electroporated the TA muscle of wild-type mice with shControl or shREDD1 plus GFP plasmid constructs. Forty-eight hours later mice were treated with a single dose of carboplatin and euthanized 5 days later. GFP positive myofibres were imaged and CSA of green fibres only was quantitated. Muscles from carboplatin-treated mice electroporated with shControl had a smaller fibre CSA compared with muscles electroporated with shREDD1, suggesting knockdown of REDD1 specifically in muscle is sufficient to attenuate carboplatin-induced muscle atrophy (*Figure 6C*). REDD1 mRNA expression was significantly increased in mouse TAs treated with carboplatin and electroporation with shREDD1 reduced REDD1 expression *in vivo* (*Figure 6D*). Our data show that muscle-specific knockdown of REDD1 both *in vitro* and *in vivo* is sufficient to attenuate chemotherapy-induced atrophy.

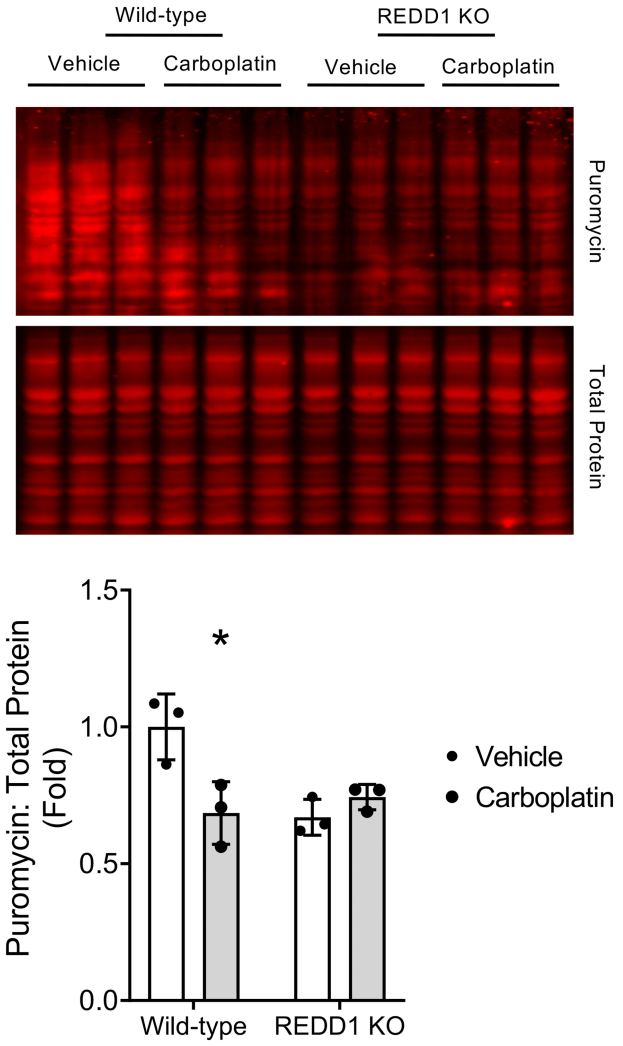

Figure 5 Loss of REDD1 attenuates carboplatin-induced protein synthesis. Puromycin incorporation *in vivo* from the TA muscle of mice treated with vehicle or carboplatin. Two-way ANOVA with Tukey's post-hoc test for multiple comparisons $*P < 0.05$. $n = 3$ biological replicates for each group.

REDD1 deletion prevents muscle weakness caused by carboplatin. Muscle function was decreased in mice treated

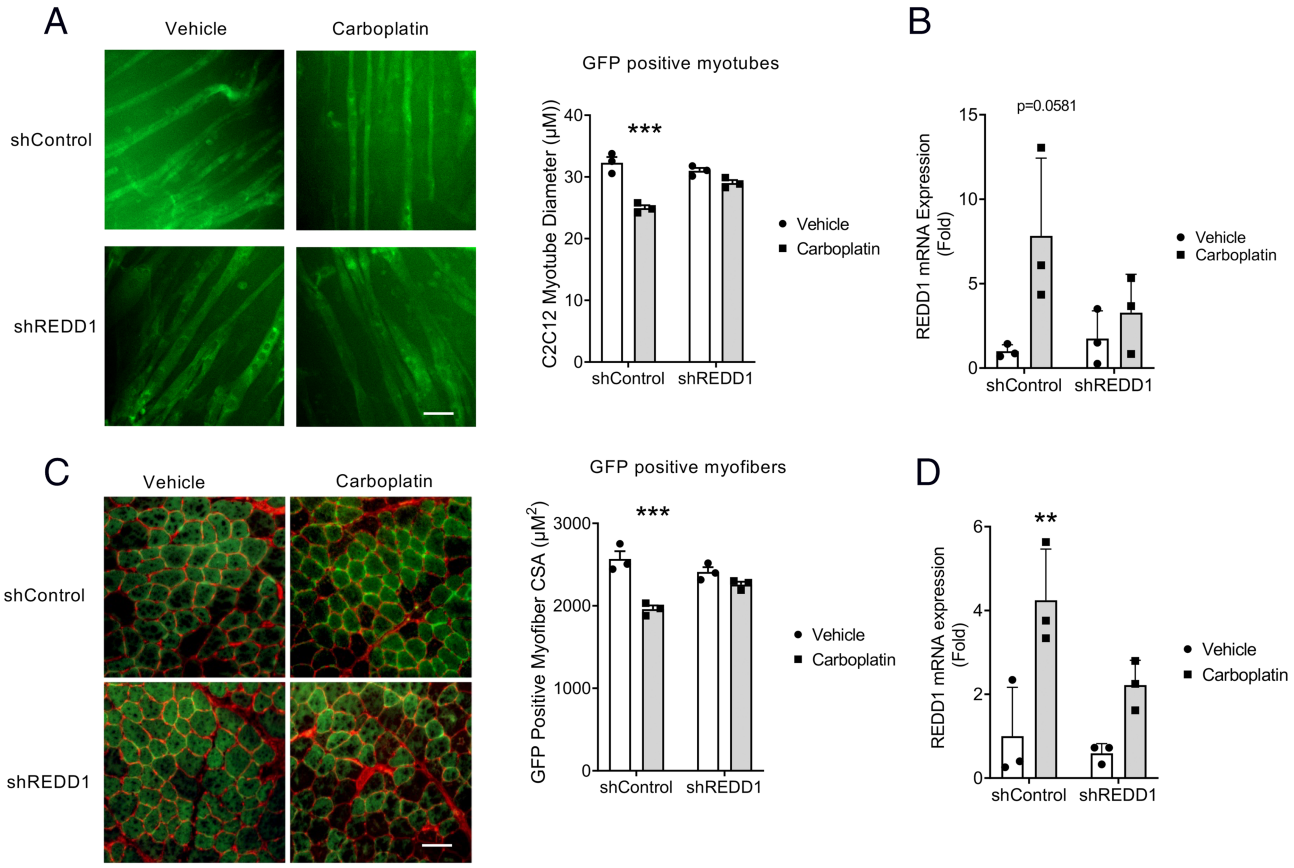

Figure 6 Knockdown of REDD1 expression both *in vitro* and *in vivo* attenuates carboplatin-induced myofibre atrophy. (*A*) Representative images of carboplatin-treated C2C12 myotubes electroporated with REDD1 shRNA or control shRNA and quantification of GFP positive myotube diameter. (*B*) REDD1 mRNA expression from C2C12 treated with carboplatin. (*C*) Representative cross sections and CSA quantification of GFP positive fibres. (*D*) REDD1 mRNA expression from the TA of carboplatin-treated mice electroporated with shControl or shREDD1. (*A–D*) Two-way ANOVA with Tukey's post-hoc test for multiple comparisons. $^{**}P < 0.01$, $^{***}P < 0.001$. n = 3 biological replicates for (*A–D*). Average myotube diameter from ~75 GFP positive myotubes per replicate (*A*). Average CSA from ~100 GFP positive fibres per replicate for (*C*). (*A*, *C*) Scale bar = 50 μm. n = 3 biological replicates for (*A–D*).

with carboplatin.[9] To determine the role of REDD1 in muscle function, we tested *in vivo* forelimb grip strength and whole muscle contractility in wild-type and REDD1 KO mice treated with carboplatin. We found that wild-type mice treated with carboplatin had decreased forelimb grip strength compared with vehicle-treated mice while REDD1 KO mice treated with carboplatin had did not have decreased grip strength (*Figure 7A*). Because forelimb grip strength is a gross measurement that can be influenced by a number of different factors including fatigue and pain, we measured whole muscle contractility in isolated EDL muscles using field stimulation. We found that absolute force was significantly decreased in wild-type mice treated with carboplatin compared with vehicle-treated mice and loss of force was completely prevented in REDD1 KO mice treated with carboplatin (*Figure 7B*). Specific force, which corrects for differences in size and weight of the muscle, was also calculated. EDL-specific force was decreased in wild-type mice treated with carboplatin compared with vehicle-treated wild-type mice. We found that while vehicle-treated REDD KO mice had decreased specific force compared with vehicle-treated wild-type mice, carboplatin did not cause a decrease of specific force of the EDL in the REDD1 KO mice (*Figure 7C*). Length of the tibia was measured for each mouse by x-ray to eliminate any influence that overall body size might have on EDL contractility, and we did not detect any difference (*Table S3*). Our data show that loss of REDD1 prevents the loss muscle function induced by carboplatin.

Discussion

Chemotherapy is essential to treat solid tumours and prevent metastasis.[1] However, many chemotherapeutic agents cause sequelae including loss of body weight, and muscle wasting

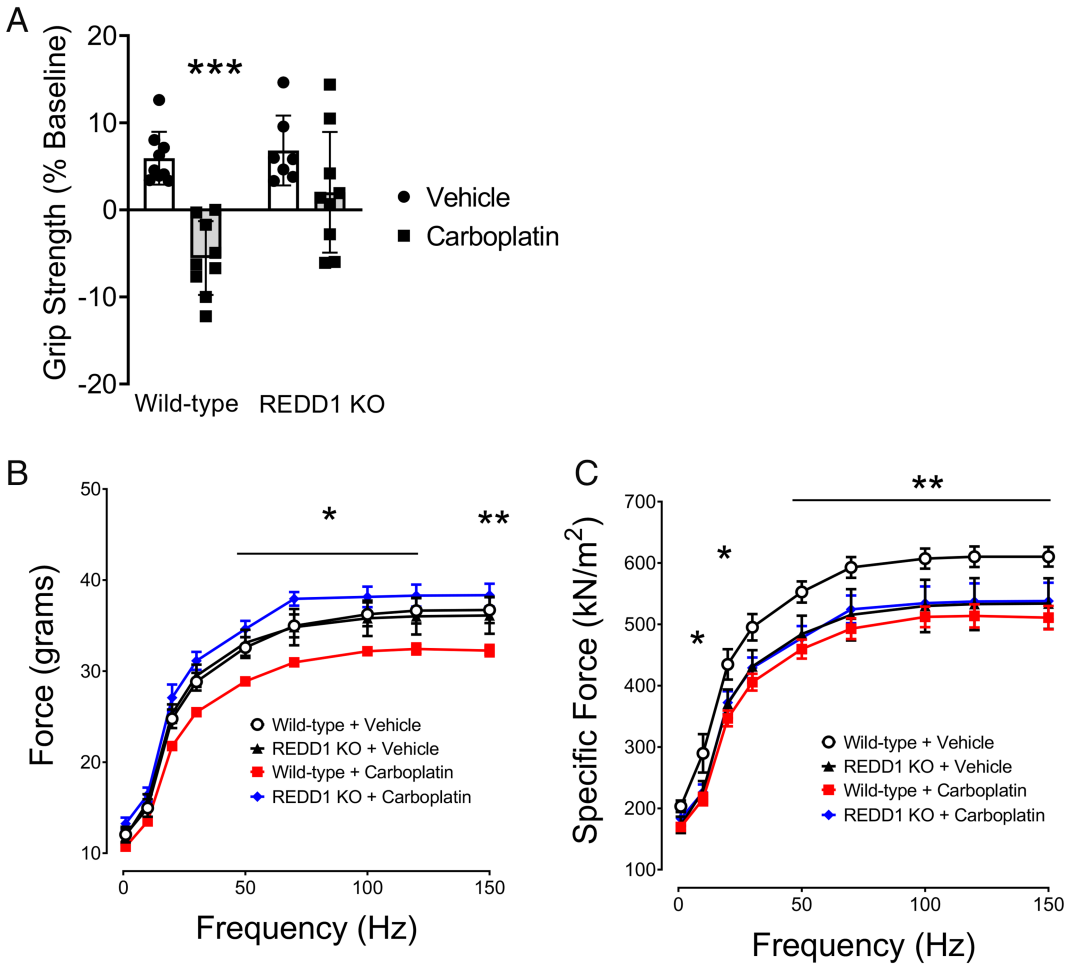

Figure 7 Loss of REDD1 prevents carboplatin-induced muscle weakness. (*A*) Deletion of REDD1 prevents carboplatin-induced forelimb grip strength reduction *in vivo*. (*B*) Absolute force generated from the EDL muscle of mice treated with vehicle or carboplatin. (*C*) Specific force of the EDL muscle of mice treated with vehicle or carboplatin. (*A–C*) Two-way ANOVA with Tukey's post-hoc test for multiple comparisons. (A) ***$P < 0.001$, compared with wild-type + vehicle. (B) *$P < 0.05$, **$P < 0.01$ all groups compared with wild-type + carboplatin. (*C*) *$P < 0.05$, **$P < 0.01$ wild-type + vehicle compared with wild-type + carboplatin $n = 8$ biological replicates for all groups.

and weakness. Maintenance of muscle mass is important for patients undergoing chemotherapy treatment in order to mitigate chemo-toxicity and maintain mobility and quality of life. Carboplatin is commonly used to treat ovarian, lung, head and neck, endometrial, oesophageal, bladder, breast, and cervical cancer. Carboplatin and other platinum-based chemotherapies interfere with DNA replication and induce cell death[47] accompanied by off-target effects including nephrotoxicity anaemia, nausea, and weakness.[48] We have previously shown that carboplatin treatment causes cachexia in mice.[8,9] While chemotherapy treatment has been shown to cause loss of muscle mass and weakness in human patients,[49,50] chemotherapy-induced muscle loss in mice occurs to a greater extent. This is a limiting factor of the study; however, REDD1 deletion is sufficient to maintain muscle mass independent of the degree of muscle loss in mice.

Expression of the stress-response protein REDD1 is significantly increased in a number of models of muscle wasting,[22,23] and its anti-anabolic effect through the inhibition of mTORC1 may play an important role in chemotherapy-induced muscle wasting. This study was designed to test whether loss of REDD1 is sufficient to prevent carboplatin-induced loss of muscle mass and muscle function.

REDD1 transcription is mediated by various transcription factors depending on the upstream stress. Hypoxia inducible factor 1 alpha has been shown to regulate REDD1 expression in response to hypoxia *in vivo*,[24] and REDD1 expression is increased in muscles from chronically hypoxic rats.[51] Another transcription factor that mediates REDD1 expression is ATF4,, a regulator of the cellular stress response. Whitney *et al*. showed that REDD1 expression was increased with tunicamycin-induced and thapsigargin-induced ER stress in C2C12 cells.[29] Additionally, Britto *et al*. show that REDD1

expression is significantly increased in muscles from mice treated with dexamethasone, a drug known to cause ER stress.[52] REDD1 is also a downstream target of p53,[53] and certain chemotherapies have been shown to activate the p53 pathway and subsequently increase REDD1 expression in response to DNA damage.[54] In this study, we found increased oxidative stress in skeletal muscle and C2C12 myotubes treated with carboplatin, and increased oxidative stress could be one mechanism of action in carboplatin chemotherapy-induced muscle loss. Cisplatin, another platinum-based chemotherapy, has been associated with increased oxidative stress through mitochondrial dysfunction in muscle[55] and oxidative stress-induced ER stress.[56] Regulated in development and DNA damage response 2 (REDD2) has also been shown to be play an important role in skeletal muscle and also inhibits mTOR signalling upon overexpression.[57] Because REDD1 was completely knocked out in the REDD1 KO mice, REDD2 may serve in a compensatory role to regulate mTOR. However, REDD2 mRNA expression in TA muscles was not significantly increased with carboplatin treatment in either wild-type or REDD1 KO mice suggesting that REDD2 is not playing a major role in compensating for loss of REDD1.

Our previous work showed that healthy mice treated with carboplatin lose body weight, muscle mass, and muscle function in as little as 7 days after a single dose.[9] In this study, we found that REDD1 KO mice treated with carboplatin did not lose as much weight as wild-type mice treated with carboplatin, but REDD1 KO did not completely prevent weight loss. Loss of total body weight is due, in part, to lower muscle weights but also depends upon a variety of factors including hydration, food intake, and adipose tissue. We previously conducted a pair-feeding study where healthy mice were fed the same amount of food as carboplatin-treated mice. We found that carboplatin-induced loss of body weight was not due to food consumption are therefore was not the primary reason for loss of weight.[9] We also weighed white adipose tissue from vehicle-treated and carboplatin-treated mice, but found no significant difference between any of the groups suggesting that changes in fat weight was not the primary cause of differences in body weight. Hydration status of the mice could also influence body weight. Indeed, mice treated with the chemotherapy drug paclitaxel had significantly lower water intake which would contribute to lower body weight; however these mice were also anorexic.[58] We have previously demonstrated that carboplatin causes decreased TA myofibre CSA[8,9] and loss of REDD1 was sufficient to maintain myofibre CSA independent of fibre type. Eight-week-old mice were used for this study based on our previous data, and these mice are skeletally mature. We measured tibia length from 8- and 12-week-old mice to confirm skeletal maturity and found no difference between the two age groups or between wild-type and REDD1 KO mice at 8 weeks of age. Additionally, 12-week-old mice treated with carboplatin lost body weight to the same extent as 8-week-old mice (*Table S3*). Regardless, loss of REDD1 was sufficient to partially attenuate carboplatin-induced loss of body weight and muscle mass.

Regulation of muscle mass is dependent upon a balance of protein synthesis and protein degradation, with muscle atrophy occurring with decreased protein synthesis and increased protein degradation.[59] While basal puromycin incorporation was lower in muscles from REDD1 KO mice treated with vehicle compared with wild-type mice, there was no further reduction of puromycin incorporation with carboplatin treatment, suggesting that loss of REDD1 prevents carboplatin-induced reduction of protein synthesis. Previous studies have also observed that basal protein synthesis in muscles from REDD1 KO mice is lower than wild-type mice and that mTORC1 signalling was not affected in REDD1 KO mice under basal conditions, suggesting that lower protein synthesis may be mTORC1-independent.[23] Steiner *et al*. postulated that reduced protein synthesis in REDD1 KO mice could provide an advantage to survival during nutrient insufficiency, although this has not been directly shown. While lower basal protein synthesis in REDD1 KO mice is of significant interest, it did not cause phenotypic changes in body weight, muscle weight, or tibia length compared with wild-type mice. While lower basal puromycin incorporation in muscles from REDD1 KO mice may obscure carboplatin-induced changes in protein synthesis, muscle mass is still maintained. There is no consensus in the literature whether or not protein synthesis is increased or decreased with chemotherapy treatment and likely depends on the type of drug, dose, frequency of administration, and health of the subject at the time of treatment. For example, one study showed that doxorubicin treatment over the course of 4 weeks caused a significant reduction of protein synthesis in conjunction with increased REDD1 expression in mice.[16] Another study showed that muscles from mice implanted with C26 tumour cells had lower rates of protein synthesis compared to non-tumour, but when treated with cystemustine, protein synthesis rates increased.[60] It is also worth noting that this study treated healthy mice with cystemustine, and a small decrease in protein synthesis was observed.[60] While more studies should be conducted with a variety of chemotherapy drugs that induce cachexia, this is the first study to show that loss of REDD1 is sufficient to prevent a decrease in protein synthesis in mice treated with chemotherapy.

Carboplatin treatment is systemic and can alter normal cell function of many off-target organ systems. In order to measure the direct effect of chemotherapy on muscle, we treated C2C12 myotubes with carboplatin and measured myotube diameter and markers of mTORC1 signalling. In agreement with previous studies, increased REDD1 expression was observed in conjunction with decreased phosphorylation of Akt threonine 308 and serine 473. Previous studies have shown that

REDD1's mechanism of action is to enhance protein phosphatase 2A's ability to dephosphorylate Akt threonine 308.[33] We also showed that carboplatin inhibits downstream markers of mTORC1 activation as well as incorporation of puromycin in agreement with our *in vivo* puromycin data. Functional and fully activated Akt is necessary for activation of mTORC1, but also serves as a nexus to both protein synthesis and protein degradation signalling by maintaining forkhead box O family's phosphorylation and sequestration to the cytosol.[61] Additionally, there is evidence that REDD1 contributes to increased autophagy in sepsis and hypoxia. Indeed, loss of REDD1 in septic mice was sufficient to maintain phosphorylation of ULK1 and prevent p62 accumulation. Loss of REDD1 also decreased sepsis-induced LC3B-II/I.[23] Because REDD1 plays a pivotal role in the regulation of Akt function and thereby mTORC1 function, loss of REDD1 may also blunt atrophic signalling as well.

Global knockout of REDD1 could complicate the skeletal muscle response due to tissue cross-talk in response to carboplatin, which could lead to indirect responses in muscle. In order to investigate a muscle-specific response, we knocked down REDD1 in carboplatin-treated C2C12 myotubes and in skeletal muscle from wild-type mice treated with carboplatin using REDD1 short hairpin RNA (shREDD1). Our data showed that muscle-specific knockdown of REDD1 is sufficient to attenuate carboplatin-induced atrophy both *in vitro* and *in vivo* (*Figure 6A–D*). REDD1 mRNA expression was not completely suppressed with shREDD1 *in vitro*, but this is likely due to low electroporation efficiency in this system. The muscle fibres or C2C12 myotubes that do not express GFP (marker for electroporation), still likely contribute to REDD1 protein expression. Only muscle fibres and C2C12 myotubes that expressed GFP were used for quantitation of CSA and myotube diameter. A limitation to this method is inefficient expression due to low electroporation, and a muscle-specific genetic knockout mouse would aid in clarifying the role of REDD1 in muscle during chemotherapy treatment. Despite this, in our hands muscle fibres and C2C12 myotubes electroporated with shREDD1 do not atrophy to the same degree as those electroporated with shControl. These data suggest that REDD1 plays an important role directly in the regulation of muscle mass during chemotherapy treatment.

Weakness and fatigue are common side effects of chemotherapy and maintaining muscle function during chemotherapy treatment improves prognosis and quality of life.[62] While our data show that REDD1 KO mice treated with carboplatin did not exhibit decreased EDL maximal tetanic specific force, the baseline contractility of EDL muscle from REDD1 KO mice was significantly decreased compared with wild-type mice. Because REDD1 KO mice have life-long loss of REDD1, it is possible that compensatory mechanisms could alter contractility in a way that we are unaware. Future studies should investigate the impact of REDD1 deletion on exercise performance including fatigue and aerobic capacity to better understand the role REDD1 plays in muscle function.

These data show that overall REDD1 plays an important role in the regulation of muscle mass in chemotherapy-induced cachexia. REDD1 is an important negative regulator of protein synthesis and loss of REDD1 significantly improves muscle mass. Further studies will be necessary to determine more precisely the mechanism of action and if this could provide potential targetable therapy for patients.

Acknowledgements

We would like to thank Elena Feinstein and Quark Pharmaceuticals, Inc. for providing the REDD1 knockout mice. We would also like to thank Michael Dennis and Allyson Toro at the Penn State College of Medicine for help with obtaining REDD1 knockout mice and colony maintenance.

Funding

This work was supported by the National Institutes of Health Grant CA205437, Phi Beta Psi Sorority, and the Pennsylvania Breast Cancer Coalition (PABCC) to D.L.W, and by a Penn State Cancer Institute Fellowship to B.A.H.

Online supplementary material

Additional supporting information may be found online in the Supporting Information section at the end of the article.

Figure S1. Carbonylated proteins from C2C12 myotubes treated with carboplatin for 24 hours and caspase 3/cleaved caspase 3 expression at 24 and 48 hours. (a) Carbonylated protein assay. (b) Caspase 3 and cleaved caspase 3 were measured from total cell lysates. (c) Caspase 3 and cleaved caspase 3 were measured from staurosporine (STP) treated C2C12 myotubes as a positive control for caspase cleavage. Quantification for colorimetric carbonyl assay (nmol/ml). Student's t-test. $*p < 0.05$. (b) Two-Way ANOVA with Tukey's post-hoc test for multiple comparisons. $****p < 0.0001$. $n = 3$ biological replicates for all groups.

Figure S2. REDD2 mRNA expression from skeletal muscle and Genotype PCR to confirm REDD1 knockout. (a) REDD2 mRNA expression in the TA from wild-type and REDD1 KO mice treated with vehicle or carboplatin. (b) Representative agarose gel showing positive REDD1 band in wild-type mice (Lane 2) and negative REDD1 band + positive neomycin band in REDD1 KO mice (Lane 3). Ear clips were used for genotyping, and each mouse used in this study was confirmed by

genotype analysis. (a) Two-way ANOVA with Tukey's post-hoc test for multiple comparisons. n = 5 biological replicates for each group.

Figure S3. Carboplatin induced body weight loss in 12-week old mice; carboplatin did not cause loss of adipose tissue; carboplatin increased carbonylated proteins in muscle. (a) Quantification of daily body weight in mice treated with carboplatin. (b) Weight of inguinal white adipose tissue (WAT) from wild-type and REDD1 KO mice treated with vehicle or carboplatin. (c) Quantification for colorimetric carbonyl assay in wild-type and REDD1 KO mice treated with carboplatin and euthanized at 5 days and normalized to mg of protein (nmol/mg). (a-c) Two-way ANOVA with Tukey's post-hoc test for multiple comparisons. $*p < 0.05$, $**p < 0.01$, $***p < 0.001$. n = 6–8 biological replicates for each group; (c) n = 4.

Table S1. Primary antibody list for Westerns and Immunofluorescence.

Table S2. List of primers for qPCR.

Table S3. Tibia Length of wild-type and REDD1 KO mice.

Conflicts of interest

All authors certify that they have complied with the ethical guidelines for authorship and publishing in the Journal of Cachexia, Sarcopenia, and Muscle.[63] This manuscript does not contain clinical studies or patient data. B.A.H, H.X., and D.L.W. claim no conflicts of interest.

References

1. Livshits Z, Rao RB, Smith SW. An approach to chemotherapy-associated toxicity. *Emerg Med Clin North Am* 2014;**32**:167–203.
2. Coletti D. Chemotherapy-induced muscle wasting: an update. *Eur J Transl Myol* 2018;**28**:7587.
3. Pin F, Couch ME, Bonetto A. Preservation of muscle mass as a strategy to reduce the toxic effects of cancer chemotherapy on body composition. *Curr Opin Support Palliat Care* 2018;**12**:420–426.
4. Cleeland CS, Allen JD, Roberts SA, Brell JM, Giralt SA, Khakoo AY, et al. Reducing the toxicity of cancer therapy: recognizing needs, taking action. *Nat Rev Clin Oncol* 2012;**9**:471–478.
5. Brown DJ, McMillan DC, Milroy R. The correlation between fatigue, physical function, the systemic inflammatory response, and psychological distress in patients with advanced lung cancer. *Cancer* 2005;**103**:377–382.
6. Galvao DA, Taaffe DR, Spry N, Joseph D, Turner D, Newton RU. Reduced muscle strength and functional performance in men with prostate cancer undergoing androgen suppression: a comprehensive cross-sectional investigation. *Prostate Cancer Prostatic Dis* 2009;**12**:198–203.
7. Barreto R, Waning DL, Gao H, Liu Y, Zimmers TA, Bonetto A. Chemotherapy-related cachexia is associated with mitochondrial depletion and the activation of ERK1/2 and p38 MAPKs. *Oncotarget* 2016;**7**:43442–43460.
8. Hain BA, Xu H, Wilcox JR, Mutua D, Waning DL. Chemotherapy-induced loss of bone and muscle mass in a mouse model of breast cancer bone metastases and cachexia. *JCSM Rapid Commun* 2019;**2**:1–12.
9. Hain BA, Jude B, Xu H, Smuin DM, Fox EJ, Elfar JC, et al. Zoledronic acid improves muscle function in healthy mice treated with chemotherapy. *J Bone Miner Res* 2020;**35**:368–381.
10. Apps MG, Choi EH, Wheate NJ. The state-of-play and future of platinum drugs. *Endocr Relat Cancer* 2015;**22**:R219–R233.
11. Sakai H, Sagara A, Arakawa K, Sugiyama R, Hirosaki A, Takase K, et al. Mechanisms of cisplatin-induced muscle atrophy. *Toxicol Appl Pharmacol* 2014;**278**:190–199.
12. Feather CE, Lees JG, Makker PGS, Goldstein D, Kwok JB, Moalem-Taylor G, et al. Oxaliplatin induces muscle loss and muscle-specific molecular changes in mice. *Muscle Nerve* 2018;**57**:650–658.
13. Conte E, Bresciani E, Rizzi L, Cappellari O, De Luca A, Torsello A, et al. Cisplatin-induced skeletal muscle dysfunction: mechanisms and counteracting therapeutic strategies. *Int J Mol Sci* 2020;**21**:1242.
14. Damrauer JS, Stadler ME, Acharyya S, Baldwin AS, Couch ME, Guttridge DC. Chemotherapy-induced muscle wasting: association with NF-κB and cancer cachexia. *Eur J Transl Myol* 2018;**28**:7590.
15. Gilliam LA, Moylan JS, Patterson EW, Smith JD, Wilson AS, Rabbani Z, et al. Doxorubicin acts via mitochondrial ROS to stimulate catabolism in C2C12 myotubes. *Am J Physiol Cell Physiol* 2012;**302**:C195–C202.
16. Nissinen TA, Degerman J, Rasanen M, Poikonen AR, Koskinen S, Mervaala E, et al. Systemic blockade of ACVR2B ligands prevents chemotherapy-induced muscle wasting by restoring muscle protein synthesis without affecting oxidative capacity or atrogenes. *Sci Rep* 2016;**6**:32695.
17. Chen J-A, Splenser A, Guillory B, Luo J, Mendiratta M, Belinova B, et al. Ghrelin prevents tumour- and cisplatin-induced muscle wasting: characterization of multiple mechanisms involved. *J Cachexia Sarcopenia Muscle* 2015;**6**:132–143.
18. Egerman MA, Glass DJ. Signaling pathways controlling skeletal muscle mass. *Crit Rev Biochem Mol Biol* 2014;**49**:59–68.
19. Bonaldo P, Sandri M. Cellular and molecular mechanisms of muscle atrophy. *Dis Model Mech* 2013;**6**:25–39.
20. Booth FW. Physiologic and biochemical effects of immobilization on muscle. *Clin Orthop Relat Res* 1987;**219**:15–20.
21. Kimball SR, Do AN, Kutzler L, Cavener DR, Jefferson LS. Rapid turnover of the mTOR complex 1 (mTORC1) repressor REDD1 and activation of mTORC1 signaling following inhibition of protein synthesis. *J Biol Chem* 2008;**283**:3465–3475.
22. Gordon BS, Williamson DL, Lang CH, Jefferson LS, Kimball SR. Nutrient-induced stimulation of protein synthesis in mouse skeletal muscle is limited by the mTORC1 repressor REDD1. *J Nutr* 2015;**145**:708–713.
23. Steiner JL, Crowell KT, Kimball SR, Lang CH. Disruption of REDD1 gene ameliorates sepsis-induced decrease in mTORC1 signaling but has divergent effects on proteolytic signaling in skeletal muscle. *Am J Physiol Endocrinol Metab* 2015;**309**:E981–E994.
24. Brugarolas J, Lei K, Hurley RL, Manning BD, Reiling JH, Hafen E, et al. Regulation of mTOR function in response to hypoxia by REDD1 and the TSC1/TSC2 tumor suppressor complex. *Genes Dev* 2004;**18**:2893–2904.
25. Gordon BS, Liu C, Steiner JL, Nader GA, Jefferson LS, Kimball SR. Loss of REDD1 augments the rate of the overload-induced increase in muscle mass. *Am J Physiol Regul Integr Comp Physiol* 2016;**311**:R545–R557.
26. Gordon BS, Steiner JL, Rossetti ML, Qiao S, Ellisen LW, Govindarajan SS, et al. REDD1 induction regulates the skeletal muscle gene expression signature following acute

aerobic exercise. *Am J Physiol Endocrinol Metab* 2017;**313**:E737–E747.
27. DeYoung MP, Horak P, Sofer A, Sgroi D, Ellisen LW. Hypoxia regulates TSC1/2-mTOR signaling and tumor suppression through REDD1-mediated 14-3-3 shuttling. *Genes Dev* 2008;**22**:239–251.
28. Shoshani T, Faerman A, Mett I, Zelin E, Tenne T, Gorodin S, et al. Identification of a novel hypoxia-inducible factor 1-responsive gene, RTP801, involved in apoptosis. *Mol Cell Biol* 2002;**22**:2283–2293.
29. Whitney ML, Jefferson LS, Kimball SR. ATF4 is necessary and sufficient for ER stress-induced upregulation of REDD1 expression. *Biochem Biophys Res Commun* 2009;**379**:451–455.
30. Black AJ, Gordon BS, Dennis MD, Jefferson LS, Kimball SR. Regulation of protein and mRNA expression of the mTORC1 repressor REDD1 in response to leucine and serum. *Biochem Biophys Rep* 2016;**8**:296–301.
31. Dibble CC, Cantley LC. Regulation of mTORC1 by PI3K signaling. *Trends Cell Biol* 2015;**25**:545–555.
32. Inoki K, Li Y, Zhu T, Wu J, Guan KL. TSC2 is phosphorylated and inhibited by Akt and suppresses mTOR signalling. *Nat Cell Biol* 2002;**4**:648–657.
33. Dennis MD, Coleman CS, Berg A, Jefferson LS, Kimball SR. REDD1 enhances protein phosphatase 2A-mediated dephosphorylation of Akt to repress mTORC1 signaling. *Sci Signal* 2014;**7**:ra68.
34. Braun TP, Szumowski M, Levasseur PR, Grossberg AJ, Zhu X, Agarwal A, et al. Muscle atrophy in response to cytotoxic chemotherapy is dependent on intact glucocorticoid signaling in skeletal muscle. *PLoS ONE* 2014;**9**:e106489.
35. Brafman A, Mett I, Shafir M, Gottlieb H, Damari G, Gozlan-Kelner S, et al. Inhibition of oxygen-induced retinopathy in RTP801-deficient mice. *Invest Ophthalmol Vis Sci* 2004;**45**:3796–3805.
36. van Hennik MB, van der Vijgh WJ, Klein I, Elferink F, Vermorken JB, Winograd B, et al. Comparative pharmacokinetics of cisplatin and three analogues in mice and humans. *Cancer Res* 1987;**47**:6297–6301.
37. Moffat J, Grueneberg DA, Yang X, Kim SY, Kloepfer AM, Hinkle G, et al. A lentiviral RNAi library for human and mouse genes applied to an arrayed viral high-content screen. *Cell* 2006;**124**:1283–1298.
38. Rana ZA, Ekmark M, Gundersen K. Coexpression after electroporation of plasmid mixtures into muscle in vivo. *Acta Physiol Scand* 2004;**181**:233–238.
39. Alzghoul MB, Gerrard D, Watkins BA, Hannon K. Ectopic expression of IGF-I and Shh by skeletal muscle inhibits disuse-mediated skeletal muscle atrophy and bone osteopenia in vivo. *FASEB J* 2004;**18**:221–223.
40. Bonetto A, Andersson DC, Waning DL. Assessment of muscle mass and strength in mice. *BoneKEy Rep* 2015;**4**:732.
41. Goodman CA, Mabrey DM, Frey JW, Miu MH, Schmidt EK, Pierre P, et al. Novel insights into the regulation of skeletal muscle protein synthesis as revealed by a new nonradioactive in vivo technique. *FASEB J* 2011;**25**:1028–1039.
42. Waning DL, Mohammad KS, Reiken S, Xie W, Andersson DC, John S, et al. Excess TGF-beta mediates muscle weakness associated with bone metastases in mice. *Nat Med* 2015;**21**:1262–1271.
43. Yamada T, Place N, Kosterina N, Ostberg T, Zhang SJ, Grundtman C, et al. Impaired myofibrillar function in the soleus muscle of mice with collagen-induced arthritis. *Arthritis Rheum* 2009;**60**:3280–3289.
44. Wen Y, Murach KA, Vechetti IJ Jr, Fry CS, Vickery C, Peterson CA, et al. MyoVision: software for automated high-content analysis of skeletal muscle immunohistochemistry. *J Appl Physiol* 2018;**124**:40–51.
45. Goodman CA, Hornberger TA. Measuring protein synthesis with SUnSET: a valid alternative to traditional techniques? *Exerc Sport Sci Rev* 2013;**41**:107–115.
46. You JS, Anderson GB, Dooley MS, Hornberger TA. The role of mTOR signaling in the regulation of protein synthesis and muscle mass during immobilization in mice. *Dis Model Mech* 2015;**8**:1059–1069.
47. Brabec V, Kasparkova J. Modifications of DNA by platinum complexes: relation to resistance of tumors to platinum antitumor drugs. *Drug Resist Updat* 2005;**8**:131–146.
48. Li R, Dalton OR, Moussa YE, Wheate NJ. The side effects of platinum-based chemotherapy drugs: a review for chemists. *Dalton Trans* 2018;**47**:6645.
49. Naito T, Okayama T, Aoyama T, Ohashi T, Masuda Y, Kimura M, et al. Skeletal muscle depletion during chemotherapy has a large impact on physical function in elderly Japanese patients with advanced non-small-cell lung cancer. *BMC Cancer* 2017;**17**:571.
50. Klassen O, Schmidt ME, Ulrich CM, Schneeweiss A, Potthoff K, Steindorf K, et al. Muscle strength in breast cancer patients receiving different treatment regimes. *J Cachexia Sarcopenia Muscle* 2017;**8**:305–316.
51. Favier FB, Costes F, Defour A, Bonnefoy R, Lefai E, Bauge S, et al. Downregulation of Akt/mammalian target of rapamycin pathway in skeletal muscle is associated with increased REDD1 expression in response to chronic hypoxia. *Am J Physiol Regul Integr Comp Physiol* 2010;**298**:R1659–R1666.
52. Britto FA, Begue G, Rossano B, Docquier A, Vernus B, Sar C, et al. REDD1 deletion prevents dexamethasone-induced skeletal muscle atrophy. *Am J Physiol Endocrinol Metab* 2014;**307**:E983–E993.
53. Ellisen LW, Ramsayer KD, Johannessen CM, Yang A, Beppu H, Minda K, et al. REDD1, a developmentally regulated transcriptional target of p63 and p53, links p63 to regulation of reactive oxygen species. *Mol Cell* 2002;**10**:995–1005.
54. Hulmi JJ, Nissinen TA, Rasanen M, Degerman J, Lautaoja JH, Hemanthakumar KA, et al. Prevention of chemotherapy-induced cachexia by ACVR2B ligand blocking has different effects on heart and skeletal muscle. *J Cachexia Sarcopenia Muscle* 2018;**9**:417–432.
55. Sirago G, Conte E, Fracasso F, Cormio A, Fehrentz JA, Martinez J, et al. Growth hormone secretagogues hexarelin and JMV2894 protect skeletal muscle from mitochondrial damages in a rat model of cisplatin-induced cachexia. *Sci Rep* 2017;**7**:13017.
56. Mandic A, Hansson J, Linder S, Shoshan MC. Cisplatin induces endoplasmic reticulum stress and nucleus-independent apoptotic signaling. *J Biol Chem* 2003;**278**:9100–9106.
57. Miyazaki M, Esser KA. REDD2 is enriched in skeletal muscle and inhibits mTOR signaling in response to leucine and stretch. *Am J Physiol Cell Physiol* 2009;**296**:C583–C592.
58. Ray MA, Trammell RA, Verhulst S, Ran S, Toth LA. Development of a mouse model for assessing fatigue during chemotherapy. *Comp Med* 2011;**61**:119–130.
59. Anthony TG. Mechanisms of protein balance in skeletal muscle. *Domest Anim Endocrinol* 2016;**56**:S23–S32.
60. Samuels SE, Knowles AL, Tilignac T, Debiton E, Madelmont JC, Attaix D. Higher skeletal muscle protein synthesis and lower breakdown after chemotherapy in cachectic mice. *Am J Physiol Regul Integr Comp Physiol* 2001;**281**:R133–R139.
61. Hay N. Interplay between FOXO, TOR, and Akt. *Biochim Biophys Acta* 2011;**1813**:1965–1970.
62. Cave J, Paschalis A, Huang CY, West M, Copson E, Jack S, et al. A systematic review of the safety and efficacy of aerobic exercise during cytotoxic chemotherapy treatment. *Support Care Cancer* 2018;**26**:3337–3351.
63. von Haehling S, Morley JE, Coats AJS, Anker SD. Ethical guidelines for publishing in the journal of cachexia, sarcopenia and muscle: update 2019. *J Cachexia Sarcopenia Muscle* 2019;**10**:1143–1145.